Author Manuscript

Author Manuscript

Author Manuscript

Author Manuscript

HHS Public Access

Author manuscript

Calcif Tissue Int. Author manuscript; available in PMC 2017 June 01.

Published in final edited form as:

Calcif Tissue Int. 2016 June ; 98(6): 619–630. doi:10.1007/s00223-016-0111-0.

Parathyroid Hormone (1–34) Transiently Protects Against Radiation-Induced Bone Fragility

Megan E. Oest[1], **Kenneth A. Mann**[1], **Nicholas D. Zimmerman**[1], and **Timothy A. Damron**[1]

[1] Department of Orthopedic Surgery, SUNY Upstate Medical University, 750 East Adams Street, Syracuse, NY 13210, USA

Abstract

Radiation therapy for soft tissue sarcoma or tumor metastases is frequently associated with damage to the underlying bone. Using a mouse model of limited field hindlimb irradiation, we assessed the ability of parathyroid hormone (1–34) fragment (PTH) delivery to prevent radiation-associated bone damage, including loss of mechanical strength, trabecular architecture, cortical bone volume, and mineral density. Female BALB/cJ mice received four consecutive doses of 5 Gy to a single hindlimb, accompanied by daily injections of either PTH or saline (vehicle) for 8 weeks, and were followed for 26 weeks. Treatment with PTH maintained the mechanical strength of irradiated femurs in axial compression for the first eight weeks of the study, and the apparent strength of irradiated femurs in PTH-treated mice was greater than that of naïve bones during this time. PTH similarly protected against radiation-accelerated resorption of trabecular bone and transient decrease in mid-diaphyseal cortical bone volume, although this benefit was maintained only for the duration of PTH delivery. Overall, PTH conferred protection against radiation-induced fragility and morphologic changes by increasing the quantity of bone, but only during the period of administration. Following cessation of PTH delivery, bone strength and trabecular volume fraction rapidly decreased. These data suggest that PTH does not negate the longer-term potential for osteoclastic bone resorption, and therefore, finite-duration treatment with PTH alone may not be sufficient to prevent late onset radiotherapy-induced bone fragility.

Keywords

Radiation; Bone; Parathyroid hormone; Bone strength; Bone morphology; Fracture

Megan E. Oest oestm@upstate.edu.

Electronic supplementary material The online version of this article (doi:10.1007/s00223-016-0111-0) contains supplementary material, which is available to authorized users.

Author Contributions MEO was responsible for study design, execution, data analysis, and manuscript preparation. KAM contributed to study design, mechanical testing methods, statistical analysis, and manuscript preparation. NDZ contributed to study execution, data collection, and manuscript editing. TAD contributed the overall study concept, advised on study design and data interpretation, and assisted with manuscript preparation. All authors have read and approved the final manuscript.

Conflict of Interest The authors have no financial or professional conflicts of interest to disclose.

Human and Animal Rights and Informed Consent All animal procedures were approved by, and performed in accordance with the ethical standards of, the SUNY Upstate Medical University Institutional Animal Care and Use Committee.

Author Manuscript Author Manuscript Author Manuscript Author Manuscript

Introduction

While radiation therapy is efficacious as a treatment for management of metastatic disease (tumor reduction, pain management) and surgical adjunct for soft tissue sarcoma, many patients will experience radiation-associated damage to normal tissues surrounding the targeted area. Inclusion of underlying bone within the irradiation field is often unavoidable, and occurs in radiotherapy treatment of breast cancers (rib), gynecologic and anorectal tumors (pelvis), and extremity soft tissue sarcomas (femur, tibia, humerus, radius, ulna) [1–7].

Skeletal morbidity following radiotherapy may include loss of trabecular bone, osteocyte death, increased bone fragility, and even bone fracture [1, 8–13]. Clinical interventions to prevent this bone damage are largely limited to radiation dose fractionation and beam collimation. Use of FDA approved pharmacologic agents, including anti-resorptive and anabolic drug therapies, could potentially provide prophylaxis against these adverse effects. Ideally, clinical interventions would prevent trabecular resorption, maintain bone strength, and preserve bone cell health.

Parathyroid hormone fragment (PTH) is used clinically in severely osteoporotic patients to shift bone homeostasis towards an anabolic state and thereby prevent fragility fractures. Off-label, it has been used to manage fracture nonunions [14, 15]. However, a black box warning for osteosarcoma based on data from early preclinical animal trials has deterred clinical application in cancer patients. The applicability of these preclinical animal data to clinical use has been challenged, and while PTH may eventually be deemed safe for use in radiotherapy patients, here we have employed PTH as a proof-of-principle treatment for its anabolic properties [16]. Specifically, we hypothesized that PTH could be used to prevent post-radiotherapy bone fragility and bone resorption, thereby maintaining bone health long term. The goal of this study was to evaluate the potential for an anabolic agent, PTH (1–34), to prevent radiation-associated bone damage using a mouse model of limited field irradiation.

Methods

Animal Model

Consistent with our previous work in this model [13, 17, 18], 98 female BALB/cJ mice (Jackson Labs, Bar Harbor, ME, aged 8 weeks on arrival and 12 weeks on first day of radiotherapy) were selected for this study, as skeletal growth has greatly slowed at this age, approximating skeletal maturity in the smallest relevant animal model. Mice were community housed (5 mice/cage, 12 h light/dark cycle) with free access to food and water, and permitted a 4-week acclimation period prior to treatment. Welfare observations were made daily throughout the 6-month study. Mice were randomly assigned to treatment groups, with $n = 7$ mice/group/time point, based on a power analysis including a 10 % standard deviation to achieve 90 % power to show a 20 % difference at a $\alpha = 0.05$.

Radiation therapy was modeled with delivery of four consecutive daily 5 Gy fractions of unilateral limited field hindlimb irradiation (4 × 5 Gy at 300 kV, BED = 55.7 $Gy_{2.8}$ using the

Author Manuscript Author Manuscript Author Manuscript Author Manuscript

linear quadratic model, Philips RT-250, Andover, MA) [19, 20]. Briefly, mice were anesthetized (ketamine/xylazine at 100/10 mg/kg IP), positioned with right hindlimbs extended into the radiation field, and a 4-mm-thick lead shield over the body and contralateral control (0 Gy) limb. In previous work with this model we did not detect any differences between non-irradiated contralateral control limbs and those derived from matched sham animals (no irradiation to either limb); therefore, no sham animals were included in this study [17]. Mice tolerated this protocol well, with no adverse events or deaths.

Beginning on the first day of radiation therapy (RTx), mice received daily subcutaneous injections for 8 weeks (5 days/week, ending at week 7 post-RTx) of either PTH (1–34) (PTH, 40 μg/kg, Sigma-Aldrich, St. Louis, MO) or an equivalent volume of vehicle (VEH, saline with carrier protein). Mice were weighed weekly and PTH or VEH dosages adjusted according to body mass. At the start of the study, mice had a mean body weight of 21.6 ± 1.9 g. The body weights of the VEH and PTH groups were not different at the start of the study (21.4 ± 2.2 and 21.8 ± 1.6 g, respectively), or at any subsequent time point. Animal behaviors, including ambulation, nutrition, activity level, and grooming, were not affected by the radiation or drug treatment. The week zero time point was defined as the day following the fourth RTx fraction. At 0, 1, 2, 4, 8, 12, and 26 weeks post-RTx, mice were euthanized and femurs were disarticulated, wrapped in saline moistened gauze, and stored at −80 °C. All methods were approved by the SUNY Upstate Institutional Animal Care and Use Committee and conducted in accordance with AAALAC guidelines.

Micro-CT Imaging

Whole femurs were imaged using micro-computed tomography (μCT 40, Scanco, Brüttisellen, Switzerland) at a 12 lm voxel resolution. Three volumes of interest (VOIs) were evaluated, including a 1-mm-thick axial section of mid-diaphyseal cortical bone (VOI shown in Fig. 2); a 0.8-mm-thick volume of metaphyseal trabecular bone located 0.4 mm proximal from the growth plate (VOI shown in Fig. 3); and cortical and trabecular bone from the distal 5 mm of the femur (VOI shown in Fig. 4). Quantitative analysis included bone volume (BV) or bone volume fraction (BV/TV), bone tissue mineral density (TMD), bone mineral content (BMC), and trabecular morphology parameters (number, thickness, spacing, connectivity, and orientation). Reconstructed 3-D images were also digitally segmented to illustrate morphologic changes (ImageJ, NIH, Bethesda, MD). The BoneJ plugin for ImageJ was used to quantify cortical wall thickness and average cortical cross-sectional area (CSA) for a 0.12-mm-thick volume of mid-diaphyseal cortical bone [21].

Mechanical Testing

Proximal femurs were potted in dental cement (COE Tray Plastic, GC America, Alsip, IL) and placed in the uniaxial test frame (Q-Test, MTS, Eden Prairie, MN). A compressive preload of 1 N was applied and the distal condyles stabilized in a 0.5-mm-deep well of dental cement. Uniaxial compression testing of the distal femur was then done at a load rate of 0.5 mm/minute until a 20 % decrease in applied load beyond peak load was reached. Outcome measures included ultimate load, work to ultimate load, and apparent strength [22].

Author Manuscript Author Manuscript Author Manuscript Author Manuscript

Apparent strength was calculated as the ultimate load divided by the apparent area of the distal 5 mm of the femur (bone volume for the distal 5 mm of the femur/5 mm).

Statistics

Morphologic and biomechanical outcome measures (dependent variables) were analyzed using two approaches. First, the effect of radiation on the outcome measures at each time point was assessed using paired t tests comparing the irradiated (right) femur to the contralateral control (left, non-irradiated) femur. To determine the effect of PTH treatment on irradiated bone, one-way ANOVAs with post hoc Tukey's tests (TT) were run at each time point for each outcome measure (JMP11, SAS, Cary, NC). The results presented here focus on the comparison between the RTx-PTH and RTx-VEH groups. In the interest of completeness, however, significant differences for the RTx-PTH vs. Ctrl-VEH and PTH-VEH vs. Ctrl-VEH are denoted in the figures.

The second analysis was done to evaluate how rates of change in the outcome measures differed between treatment groups over time using Analysis of Covariance (ANCOVA, with time as the covariate). For the ANCOVA analyses, a log transformation was performed on the time scale for 0–12 week time points to linearize the response; 26-week data were excluded to isolate the main effects of the PTH treatment (delivered during weeks 0–7 of the study). To evaluate the RTx model used in this study, ANCOVA was used to test whether RTx (RTx-VEH group) had a different effect on the outcome measures over time compared to control bones (Ctrl-VEH group). To evaluate whether PTH could ameliorate the effects of RTx, ANCOVA was used to test whether PTH (RTx-PTH group) altered the response over time compared to the group receiving the RTx regime (RTx-VEH group). Differences in slope could be assessed using the interaction term of the ANCOVA. For all outcomes, statistical significance was defined at $p \leq 0.05$. The final samples sizes analyzed were $n = 6$–7 mice/group/time point after excluding samples that fell outside of a 95 % confidence interval.

Results

Micro-CT Imaging

Gross visual examination of the reconstructed micro-CT images, in addition to quantitative analyses, visibly illustrated radiation and PTH treatment effects. Both sagittal and metaphyseal transverse image sections illustrate the loss of trabecular bone in irradiated femurs (Fig. 1). PTH treatment prevented the apparent loss of trabecular bone in irradiated femurs at weeks two and four. Femurs from the RTx-PTH group, however, showed more extensive loss of trabecular bone following cessation of PTH (weeks 8–12) than Ctrl-PTH femurs.

Mid-Diaphyseal Cortex—Both cortical BV and BMC were significantly decreased by radiation in the VEH group (VEH-RTx vs. VEH-Ctrl) at 4- to 26-week time points (Fig. 2a, b, $t \leq 0.049$ by paired t tests), and significantly increased at week 26 ($t < 0.039$ by paired t test). Cortical TMD was increased in VEH-RTx samples compared to VEH-Ctrl at week 2, and decreased at weeks 12 and 26 (Fig. 2c, all $t \leq 0.031$ by paired t tests). Results for cross-

Author Manuscript Author Manuscript Author Manuscript Author Manuscript

sectional area (CSA) and mean cortical thickness are summarized in Supplementary Table 1. An ANCOVA comparing Ctrl-VEH and RTx-VEH groups between 0 and 12 weeks showed that while mean cortical thickness increased over time in control femurs, it remained constant in irradiated femurs, with the rate of change significantly different between the two groups (Table 1; Fig. 6a, $p < 0.009$).

Cortical bone volume was significantly increased in PTH-RTx femurs compared to VEH-RTx at week 8 (Fig. 2A, $p < 0.001$ by TT). Bone mineral content (Fig. 2b) was similarly increased in the PTH-RTx group compared to VEH-RTx at week 8 ($p < 0.001$ by TT). Mid-diaphyseal cortical tissue mineral density was not different between PTH-RTx and VEH-RTx groups at any time point. Using an ANCOVA to compare RTx-VEH and RTx-PTH samples over the 0- to 12-week time points demonstrated that PTH significantly increased cortical BV, BMC, CSA, and mean thickness in irradiated bones (Table 1, $p < 0.001$). The rate of increase was also significantly greater ($p \leq 0.020$) in RTx-PTH samples than RTx-VEH samples for the diaphyseal BV, BMC, CSA (Table 1), and mean cortex thickness (Fig. 6b).

Metaphyseal Trabecular Bone—Trabecular bone volume fraction (BV/TV, Fig. 3a) was initially increased by RTx in the VEH group at weeks 0–1 ($t \leq 0.039$ by paired t tests), but decreased by RTx thereafter ($t < 0.038$ at weeks 4–12, with $t = 0.055$ at week 26). Trabecular number (Tb.N, Fig. 3b) was transiently increased in RTx samples from the VEH group ($t = 0.004$ vs. VEH-Ctrl at week 0), and later decreased ($t < 0.001$ at weeks 2–4 and $t = 0.088$ at week 12, all by paired t tests). There was substantial variability in the trabecular number, thickness, and spacing for the irradiated samples in the VEH group at week 26, as three of seven femurs were completely devoid of trabecular structures. Tissue mineral density (TMD, Fig. 3c) was significantly increased at weeks 0, 1, 4, and 8 in VEH-RTx samples compared to VEH-Ctrl samples ($t \leq 0.020$). Trabecular thickness (Tb.Th, Supplementary Table 2) was increased in VEH-RTx samples compared to controls at weeks 1–4 ($t \leq 0.024$) and decreased at week 12 ($t < 0.010$), while trabecular spacing (Tb.Sp) was increased at 0, 2, 4, and 12 weeks ($t \leq 0.004$). Additional trabecular morphology parameters are summarized in Supplementary Table 2. An ANCOVA comparing Ctrl-VEH and RTx-VEH data over weeks 0–12 found that RTx significantly accelerated the rate of trabecular bone loss, as measured by rate of decrease in BV/TV (Fig. 6c), Tb.N, and connectivity density (Conn.D, Table 1, $p < 0.001$ for all three) parameters. RTx also accelerated the rate of increase in trabecular spacing and structural model index (SMI) compared to non-irradiated controls ($p < 0.002$).

Metaphyseal BV/TV was significantly increased in PTH-RTx femurs compared to VEH-RTx femurs at weeks 1–8 (Fig. 3a, $p \leq 0.001$ by TT). Trabecular number significantly increased in PTH-RTx femurs at weeks 1–2 (Fig. 3b, $p \leq 0.006$ vs. VEH-RTx by TT, with $p = 0.057$ at week 4). Tissue mineral density was significantly increased in PTH-RTx femurs compared to VEH-RTx femurs only at week 26 (Fig. 3c, $p < 0.009$). At weeks 1–8 and 26, Tb.Th was significantly increased in the PTH-RTx group compared to VEH-RTx ($p < 0.014$ by TT, Supplementary Table 2), and Tb.Sp significantly decreased at weeks one and two ($p \leq 0.035$ by TT). Using an ANCOVA to compare RTx-VEH and RTx-PTH groups between 0 and 12 weeks, PTH was found to significantly increase BV/TV (Fig. 6d), Tb.N, Tb.Th, and

Author Manuscript Author Manuscript Author Manuscript Author Manuscript

Conn.D in irradiated bones ($p < 0.001$), while decreasing Tb.Sp and SMI (Table 1, $p < 0.001$). With the exception of SMI ($p = 0.034$), the rate of change in these parameters was not different between the PTH-RTx and VEH-RTx groups.

Distal Femur—Bone volume in the distal femur (Fig. 4a) was significantly increased in the VEH-RTx femurs compared to VEH-Ctrl femurs at 0–12 weeks ($t \leq 0.040$ by paired t tests). Similarly, distal femur BMC (Fig. 4b) increased in VEH-RTx femurs compared to VEH-Ctrl femurs at weeks 0–12 ($t < 0.048$ by paired t tests). Tissue mineral density (Fig. 4c) over this region was increased in VEH-RTx samples at weeks four and eight post-RTx ($t \leq 0.047$ vs. VEH-Ctrl by paired t tests). Using an ANCOVA to compare Ctrl-VEH and RTx-VEH samples between 0 and 12 weeks post-RTx, radiation treatment significantly increased mean BV and BMC, but did not significantly affect the rate of change in BV (Fig. 6e) or BMC (Table 1). The rate of increase in TMD, however, was significantly elevated ($p = 0.003$) in RTx-VEH samples compared to Ctrl-VEH.

Irradiated femurs in PTH-treated mice demonstrated increased bone volume at weeks 0–12 compared to VEH-RTx femurs (Fig. 4a, $p \leq 0.045$ by TT). BMC followed the response of BV, and was increased in the PTH-RTx samples at weeks 0–12 (Fig. 4b, $p \leq 0.003$ vs. VEH-RTx except for week 2, where $p = 0.075$ by TT). Tissue mineral density (Fig. 4c) was increased in the PTH-RTx group at weeks 2–4 ($p < 0.030$ vs. VEH-RTx). ANCOVA comparison of RTx-VEH and RTx-PTH samples between 0 and 12 weeks revealed that PTH treatment of irradiated bones significantly increased BV and BMC at the distal femur, while significantly decreasing TMD (Table 1). The rate of increase in BV (Fig. 6f) and BMC values was significantly greater ($p < 0.007$) in the RTx-PTH group than in the RTx-VEH group.

Mechanical Testing

Ultimate load (Fig. 5a) was initially increased in response to radiation ($t \leq 0.011$ for VEH-RTx vs. VEH-Ctrl at week 1 by paired t test). Following this, VEH-RTx femurs demonstrated decreased ultimate load compared to VEH-Ctrl femurs at week 8 ($t < 0.017$, with $t = 0.059$ at week 12 by paired t tests). Apparent strength (Fig. 5b) was significantly decreased in the VEH-RTx group compared to VEH-Ctrl at weeks 2, 8, and 12 ($t < 0.0325$ by paired t tests). Work to ultimate load (Fig. 5c) increased at weeks 0–1 in the VEH-RTx group ($t < 0.006$ vs. VEH-Ctrl by paired t tests), and then decreased at weeks 8–24 ($t \leq 0.022$ vs. VEH-Ctrl by paired t tests). Stiffness was significantly increased at week 12 ($t < 0.001$, Supplementary Table 3). Comparison of Ctrl-VEH and RTx-VEH groups over weeks 0–12 by ANCOVA showed that RTx decreased apparent strength (Table 1, $p < 0.014$). The rate of increase for stiffness ($p < 0.001$), and rate of decrease for ultimate load, work to ultimate load, and apparent strength (Fig. 6g) was significantly greater in the RTx-VEH group than the Ctrl-VEH group ($p \leq 0.012$).

PTH treatment significantly increased ultimate load in irradiated femurs at weeks 0–8 (Fig. 5a, $p \leq 0.018$ for PTH-RTx vs. VEH-RTx by TT). Apparent strength in PTH-RTx femurs increased compared to VEH-RTx femurs at weeks 1, 4, and 8 (Fig. 5b, $p \leq 0.040$ by TT). Work to ultimate load was increased at weeks 0–8 in PTH-RTx femurs (Fig. 5c, $p \leq 0.026$

Author Manuscript Author Manuscript Author Manuscript Author Manuscript

vs. VEH-Ctrl by TT). Using ANCOVA to compare RTx-VEH samples to RTx-PTH samples over weeks 0–12 (Table 1) indicated that PTH treatment significantly increased ultimate load, work to ultimate load, and apparent strength (Fig. 6h) in irradiated samples ($p < 0.001$). PTH treatment did not modify the rate of change in these parameters in irradiated bones.

Discussion

Consistent with previous observations in this model of limited field irradiation, radiation-induced bone fragility was characterized by a biphasic (initial increase then decrease) change in apparent strength, and an accelerated loss of mechanical integrity (ultimate load, work, apparent strength) [22]. Trabecular architecture changes also followed a biphasic response, with an initial increase in trabecular BV/TV followed by accelerated rate of trabecular resorption (decreased BV/TV, increased Tb.Sp). There was increased trabecular TMD, and increased distal femur bone volume with time, but overall loss of mechanical strength following radiation treatment, suggesting that there was damage to the bone tissue making it more brittle. It is well established that bone strength is not determined wholly by bone quantity [23]. Rather, the strength of bone is derived from the interaction between morphology (including quantity) and tissue quality [24]. Increased bone quantity may temporally correlate with decreased bone strength, if the bone matrix is of poor quality. In this model, bone fragility may result from both direct radiation damage to the matrix quality (e.g., collagen cross-linking) and cell-mediated alterations of matrix quantity and quality (e.g., trabecular resorption).

In this model, PTH treatment was effective in amelio-rating bone damage during the first 8–12 weeks following radiation. PTH prevented radiation-induced loss of trabecular bone, cortical bone volume, and mechanical strength over the first 8–12 weeks post-RTx. In irradiated bones, the rate of trabecular bone loss between 0 and 12 weeks was not different between VEH and PTH groups, but the PTH groups on average had more trabecular bone. The increased quantity of trabecular bone in PTH-treated samples may have offset the time before which RTx-associated damage becomes critical. Given similar rates of resorption, starting with more bone would prolong the amount of time before the trabecular bone is completely resorbed. Bone mineral density was not consistently increased by PTH delivery, likely due to the rapid formation of new bone induced by anabolic drug delivery. Cessation of PTH treatment was followed by remodeling of the bone formed in response to the drug delivery. This was expected following discontinuation of an anabolic stimulus, and the known ability of PTH to potentiate osteoclastic activity [25].

While PTH treatment preserved trabecular bone in irradiated specimens up to 8 weeks post-RTx, discontinuation of PTH was followed by a rapid decrease in metaphyseal BV/TV between 8 and 12 weeks. This extensive trabecular bone resorption implies a corresponding increase in osteoclast numbers or activity. This was an unexpected finding, since in our previous work with this same animal model of limited field radiotherapy, we documented increased osteoclast numbers at 2–4 weeks post-RTx, followed by persistent long-term depletion of osteoclasts [13]. Future work could verify the relationship between this rapid

Author Manuscript Author Manuscript Author Manuscript Author Manuscript

post-PTH loss of trabecular structure and local osteoclast activity in irradiated hindlimbs through histology and histomorphometry.

The literature suggests that PTH can promote post-radiation survival of hematopoietic lineage cells, potentially preserving the osteoclast progenitor population. PTH is known to promote hematopoietic progenitor cell survival if delivered within a few hours of radiation exposure [26, 27]. Additionally, PTH has been shown to increase osteoclast progenitor populations in vivo and potentiate osteoclastic activity, although this has only been demonstrated following shorter durations of PTH dosing [28]. It is possible that, in this model, PTH treatment preserved osteoclast progenitor cell populations from radiation damage, and permitted or even potentiated increased osteoclast activity following discontinuation of PTH injections.

PTH treatment in this model was not, however, entirely without long-term benefit. In irradiated bones, the 8-week PTH treatment resulted in higher metaphyseal BV/TV and TMD at 26 weeks. By 26 weeks, the treatment groups had converged towards Ctrl-VEH values for many outcome measures. Interpretation of the 26-week data is also complicated by normal age-associated bone loss in older mice (here, aged 9.5 months) [29].

Other groups have documented the efficacy of PTH delivery in lessening osteolytic tumor damage in irradiated bone, augmenting distraction osteogenesis in irradiated mandibles, preventing early trabecular bone loss following low-dose irradiation of juvenile rat hindlimbs, and maintaining osteocyte viability following focal radiotherapy [30–34]. Most published studies evaluating PTH in orthopedic radiation damage models have delivered the drug for the entire duration between irradiation and the final end-point, or not sampled multiple time points [31–35]. The study presented here represents, to our knowledge, the first long-term evaluation of finite-duration PTH treatment as an adjunct to limited field irradiation in an animal model.

Radiation damage to bone may manifest through multiple processes, including both direct damage to the bone matrix as well as cell-mediated processes. Direct damage to the bone matrix by ionizing radiation may include decreased mineralization, altered mineral-to-matrix ratio, pathologic matrix cross-linking, and collagen fragmentation [17, 36, 37]. Focal radiation (5 × 4 Gy) has been shown both to decrease local osteoblast and osteoclast numbers, and to reduce marrow progenitor cell (MPC) self-renewal and osteoblastic differentiation capabilities in a mouse model [38]. In addition to depleting hematopoietic progenitor cell (HPC) populations, radiation may indirectly suppress HPC proliferation through increased marrow adiposity [37, 39, 40]. Radiation can also damage progenitor stem cell populations through direct destruction of bone vasculature, which is critical for maintenance of the stem cell niches [38].

Our results suggest that deriving long-term clinical benefit from PTH as a radiotherapy adjunct may require further untangling of the complex mechanisms involved in PTH signaling. Regulation of hematopoietic cell viability and proliferation by PTH is thought to occur through direct PTH activity on marrow progenitors or osteoblast lineage cells, although the specific cell type is yet unidentified [25, 28, 41]. Similarly, the anabolic activity

Author Manuscript Author Manuscript Author Manuscript Author Manuscript

of PTH is associated with increased hematopoietic marrow cell numbers and increased MPC proliferative potential, possibly controlled through PTH upregulation of TGFb signaling [35, 41]. The ability of PTH to act as both an anabolic agent (intermittent delivery) and catabolic agent (continuous delivery) reflects the complexity of in vivo PTH signaling, which appears to be regulated through the interactions of multiple marrow cell populations [42–44]. While intermittent PTH delivery exerts an overall anabolic effect, PTH-induced osteoblastogenesis is accompanied by an overall increase in RANKL expression by the osteoblasts, possibly potentiating osteoclast differentiation or activity [28, 45]. In order to maintain long-term bone health and homeostasis following radiotherapy, preservation of both hematopoietic/osteoclast and mesenchymal/osteoblast lineage cells would be necessary.

Conclusions

Bone damage following radiotherapy is characterized by diverse, site-specific, and time-dependent responses to mechanical properties and morphology [13, 22]. In this mouse model, radiation induces morphologic alterations at the distal femur, accelerated loss of trabecular structures, and an early increase in mechanical strength followed by a later decrease. Delivery of PTH (1–34) protected against loss of bone strength and trabecular structures not by slowing the rate at which bone was resorbed, but by providing more initial material to be lost. Interestingly, the benefits of PTH therapy on bone strength and trabecular architecture were rapidly lost following cessation of drug delivery. Had mice received PTH for the duration of this 6-month study, these parameters would likely have been maintained in the PTH-RTx group. Further investigation is necessary to identify potential strategies for maintaining the beneficial effects of PTH in irradiated bone following cessation of PTH treatment, as indefinite delivery of parathyroid hormone is clinically contraindicated.

Supplementary Material

Refer to Web version on PubMed Central for supplementary material.

Acknowledgments

This study was funded by the National Institute of Arthritis and Musculoskeletal and Skin Diseases (NIAMS) of the National Institutes of Health under award number AR065419, and by the David G. Murray Endowment (SUNY Upstate Medical University). The content is solely the responsibility of the authors and does not necessarily represent the official views of the National Institutes of Health.

References

1. Baxter NN, Habermann EB, Tepper JE, Durham SB, Virnig BA. Risk of pelvic fractures in older women following pelvic irradiation. JAMA. 2005; 294:2587–2593. [PubMed: 16304072]
2. Oh D, Huh SJ, Nam H, Park W, Han Y, do Lim H, Ahn YC, Lee JW, Kim BG, Bae DS, Lee JH. Pelvic insufficiency fracture after pelvic radiotherapy for cervical cancer: analysis of risk factors. Int J Radiat Oncol Biol Phys. 2008; 70:1183–1188. [PubMed: 17919836]
3. Voroney JP, Hope A, Dahele MR, Purdie TG, Franks KN, Pearson S, Cho JB, Sun A, Payne DG, Bissonnette JP, Bezjak A, Brade AM. Chest wall pain and rib fracture after stereotactic radiotherapy for peripheral non-small cell lung cancer. J Thorac Oncol. 2009; 4:1035–1037. [PubMed: 19633478]
4. Park SH, Kim JC, Lee JE, Park IK. Pelvic insufficiency fracture after radiotherapy in patients with cervical cancer in the era of PET/CT. Radiat Oncol J. 2011; 29:269–276. [PubMed: 22984680]

Author Manuscript Author Manuscript Author Manuscript Author Manuscript

5. Dunlap NE, Cai J, Biedermann GB, Yang W, Benedict SH, Sheng K, Schefter TE, Kavanagh BD, Larner JM. Chest wall volume receiving [30 Gy predicts risk of severe pain and/or rib fracture after lung stereotactic body radiotherapy. Int J Radiat Oncol Biol Phys. 2010; 76:796–801. [PubMed: 19427740]
6. Helmstedter CS, Goebel M, Zlotecki R, Scarborough MT. Pathologic fractures after surgery and radiation for soft tissue tumors. Clin Orthop Relat Res. 2001; 389:165–172. [PubMed: 11501806]
7. Holt GE, Griffin AM, Pintilie M, Wunder JS, Catton C, O'Sullivan B, Bell RS. Fractures following radiotherapy and limb-salvage surgery for lower extremity soft-tissue sarcomas. A comparison of high-dose and low-dose radiotherapy. J Bone Joint Surg Am. 2005; 87:315–319. [PubMed: 15687153]
8. Bandstra ER, Pecaut MJ, Anderson ER, Willey JS, De Carlo F, Stock SR, Gridley DS, Nelson GA, Levine HG, Bateman TA. Long-term dose response of trabecular bone in mice to proton radiation. Radiat Res. 2008; 169:607–614. [PubMed: 18494551]
9. Hamilton SA, Pecaut MJ, Gridley DS, Travis ND, Bandstra ER, Willey JS, Nelson GA, Bateman TA. A murine model for bone loss from therapeutic and space-relevant sources of radiation. J Appl Physiol. 2006; 101:789–793. [PubMed: 16741258]
10. Willey JS, Livingston EW, Robbins ME, Bourland JD, Tirado-Lee L, Smith-Sielicki H, Bateman TA. Risedronate prevents early radiation-induced osteoporosis in mice at multiple skeletal locations. Bone. 2010; 46:101–111. [PubMed: 19747571]
11. Willey JS, Lloyd SA, Robbins ME, Bourland JD, Smith-Sielicki H, Bowman LC, Norrdin RW, Bateman TA. Early increase in osteoclast number in mice after whole-body irradiation with 2 Gy X rays. Radiat Res. 2008; 170:388–392. [PubMed: 18763868]
12. Guise TA. Bone loss and fracture risk associated with cancer therapy. Oncologist. 2006; 11:1121–1131. [PubMed: 17110632]
13. Oest ME, Franken V, Kuchera T, Strauss J, Damron TA. Long-term loss of osteoclasts and unopposed cortical mineral apposition following limited field irradiation. J Orthop Res. 2014; 33:334–342. [PubMed: 25408493]
14. Oteo-Alvaro A, Moreno E. Atrophic humeral shaft non-union treated with teriparatide (rh PTH 1-34): a case report. J Shoulder Elbow Surg. 2010; 19:22–28.
15. Paridis D, Karachalios T. Atrophic femoral bone nonunion treated with 1-84 PTH. J Musculoskelet Neuronal Interact. 2011; 11:320–322. quiz 323. [PubMed: 22130141]
16. Subbiah V, Madsen VS, Raymond AK, Benjamin RS, Ludwig JA. Of mice and men: divergent risks of teriparatide-induced osteosarcoma. Osteoporos Int. 2010; 21:1041–1045. [PubMed: 19597911]
17. Gong B, Oest ME, Mann KA, Damron TA, Morris MD. Raman spectroscopy demonstrates prolonged alteration of bone chemical composition following extremity localized irradiation. Bone. 2013; 57:252–258. [PubMed: 23978492]
18. Oest ME, Damron TA. Focal therapeutic irradiation induces an early transient increase in bone glycation. Radiat Res. 2014; 181:439–443. [PubMed: 24701964]
19. Fowler JF. 21 years of biologically effective dose. Br J Radiol. 2010; 83:554–568. [PubMed: 20603408]
20. Hopewell JW. Radiation-therapy effects on bone density. Med Pediatr Oncol. 2003; 41:208–211. [PubMed: 12868120]
21. Doube M, Klosowski MM, Arganda-Carreras I, Cordelieres FP, Dougherty RP, Jackson JS, Schmid B, Hutchinson JR, Shefelbine SJ. BoneJ: free and extensible bone image analysis in ImageJ. Bone. 2010; 47:1076–1079. [PubMed: 20817052]
22. Wernle JD, Damron TA, Allen MJ, Mann KA. Local irradiation alters bone morphology and increases bone fragility in a mouse model. J Biomech. 2010; 43:2738–2746. [PubMed: 20655052]
23. van der Meulen MC, Jepsen KJ, Mikic B. Understanding bone strength: size isn't everything. Bone. 2001; 29:101–104. [PubMed: 11502469]
24. Jepsen K. Functional interactions among morphologic and tissue quality traits define bone quality. Clin Orthop Relat Res. 2011; 469:2150–2159. [PubMed: 21125361]

Author Manuscript Author Manuscript Author Manuscript Author Manuscript

25. Li X, Qin L, Bergenstock M, Bevelock LM, Novack DV, Partridge NC. Parathyroid hormone stimulates osteoblastic expression of MCP-1 to recruit and increase the fusion of pre/ osteoclasts. J Biol Chem. 2007; 282:33098–33106. [PubMed: 17690108]

26. Whitfield JF. Parathyroid hormone (PTH) and hematopoiesis: new support for some old observations. J Cell Biochem. 2005; 96:278–284. [PubMed: 16088941]

27. Whitfield JF. Parathyroid hormone: a novel tool for treating bone marrow depletion in cancer patients caused by chemotherapeutic drugs and ionizing radiation. Cancer Lett. 2006; 244:8–15. [PubMed: 16540235]

28. Jacome-Galarza CE, Lee SK, Lorenzo JA, Aguila HL. Parathyroid hormone regulates the distribution and osteoclastogenic potential of hematopoietic progenitors in the bone marrow. J Bone Miner Res. 2011; 26:1207–1216. [PubMed: 21611963]

29. Jilka RL. The relevance of mouse models for investigating age-related bone loss in humans. J Gerotol A Biol Sci Med Sci. 2013; 68:1209–1217.

30. Arrington SA, Fisher ER, Willick GE, Mann KA, Allen MJ. Anabolic and antiresorptive drugs improve trabecular microarchitecture and reduce fracture risk following radiation therapy. Calcif Tissue Int. 2010; 87:263–272. [PubMed: 20563797]

31. Deshpande SS, Gallagher KK, Donneys A, Tchanque-Fossuo CN, Sarhaddi D, Nelson NS, Chepeha DB, Buchman SR. Parathyroid hormone therapy mollifies radiation-induced biomechanical degradation in murine distraction osteogenesis. Plast Reconstr Surg. 2013; 132:91e–100e.

32. Gallagher KK, Deshpande S, Tchanque-Fossuo CN, Donneys A, Sarhaddi D, Nelson NS, Chepeha DB, Buchman SR. Role of parathyroid hormone therapy in reversing radiation-induced nonunion and normalization of radiomorphometrics in a murine mandibular model of distraction osteogenesis. Head Neck. 2013; 35:1732–1737. [PubMed: 23335324]

33. Chandra A, Lan S, Zhu J, Lin T, Zhang X, Siclari VA, Altman AR, Cengel KA, Liu XS, Qin L. PTH prevents the adverse effects of focal radiation on bone architecture in young rats. Bone. 2013; 55:449–457. [PubMed: 23466454]

34. Chandra A, Lin T, Tribble MB, Zhu J, Altman AR, Tseng WJ, Zhang Y, Akintoye SO, Cengel K, Liu XS, Qin L. PTH1-34 alleviates radiotherapy-induced local bone loss by improving osteoblast and osteocyte survival. Bone. 2014; 67:33–40. [PubMed: 24998454]

35. Koh AJ, Novince CM, Li X, Wang T, Taichman RS, McCauley LK. An irradiation-altered bone marrow microenvironment impacts anabolic actions of PTH. Endocrinology. 2011; 152:4525–4536. [PubMed: 22045660]

36. Acil Y, Springer IN, Niehoff P, Gassling V, Warnke PH, Acmaz S, Sonmez TT, Kimmig B, Lefteris V, Wiltfang J. Proof of direct radiogenic destruction of collagen in vitro. Strahlenther Onkol. 2007; 183:374–379. [PubMed: 17609870]

37. Green DE, Adler BJ, Chan ME, Lennon JJ, Acerbo AS, Miller LM, Rubin CT. Altered composition of bone as triggered by irradiation facilitates the rapid erosion of the matrix by both cellular and physicochemical processes. PLoS One. 2013; 8:e64952. [PubMed: 23741433]

38. Cao X, Wu X, Frassica D, Yu B, Pang L, Xian L, Wan M, Lei W, Armour M, Tryggestad E, Wong J, Wen CY, Lu WW, Frassica FJ. Irradiation induces bone injury by damaging bone marrow microenvironment for stem cells. Proc Natl Acad Sci USA. 2011; 108:1609–1614. [PubMed: 21220327]

39. Green DE, Rubin CT. Consequences of irradiation on bone and marrow phenotypes, and its relation to disruption of hematopoietic precursors. Bone. 2014; 63C:87–94. [PubMed: 24607941]

40. Naveiras O, Nardi V, Wenzel PL, Hauschka PV, Fahey F, Daley GQ. Bone-marrow adipocytes as negative regulators of the haematopoietic microenvironment. Nature. 2009; 460:259–263. [PubMed: 19516257]

41. Calvi LM, Adams GB, Weibrecht KW, Weber JM, Olson DP, Knight MC, Martin RP, Schipani E, Divieti P, Bringhurst FR, Milner LA, Kronenberg HM, Scadden DT. Osteoblastic cells regulate the haematopoietic stem cell niche. Nature. 2003; 425:841–846. [PubMed: 14574413]

42. Calvi LM, Bromberg O, Rhee Y, Weber JM, Smith JN, Basil MJ, Frisch BJ, Bellido T. Osteoblastic expansion induced by parathyroid hormone receptor signaling in murine osteocytes is not

Author Manuscript Author Manuscript Author Manuscript Author Manuscript

sufficient to increase hematopoietic stem cells. Blood. 2012; 119:2489–2499. [PubMed: 22262765]

43. Charles JF, Aliprantis AO. Osteoclasts: more than ‘bone eaters’. Trends Mol Med. 2014; 20:449–459. [PubMed: 25008556]
44. Huber BC, Grabmaier U, Brunner S. Impact of parathyroid hormone on bone marrow-derived stem cell mobilization and migration. World J Stem Cells. 2014; 6:637–643. [PubMed: 25426261]
45. Lee SK, Lorenzo JA. Parathyroid hormone stimulates TRANCE and inhibits osteoprotegerin messenger ribonucleic acid expression in murine bone marrow cultures: correlation with osteoclast-like cell formation. Endocrinology. 1999; 140:3552–3561. [PubMed: 10433211]

Author Manuscript Author Manuscript Author Manuscript Author Manuscript

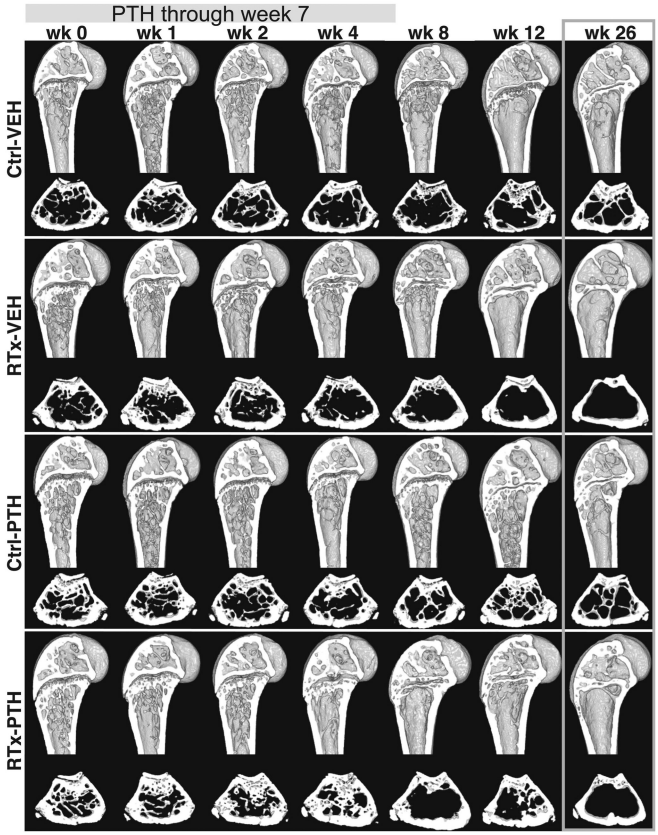

Fig. 1.

Digitally sectioned views of the distal femurs at each time point, including sagittal sections of the distal 5 mm of the femur and transverse sections through the metaphysis

Author Manuscript Author Manuscript Author Manuscript Author Manuscript

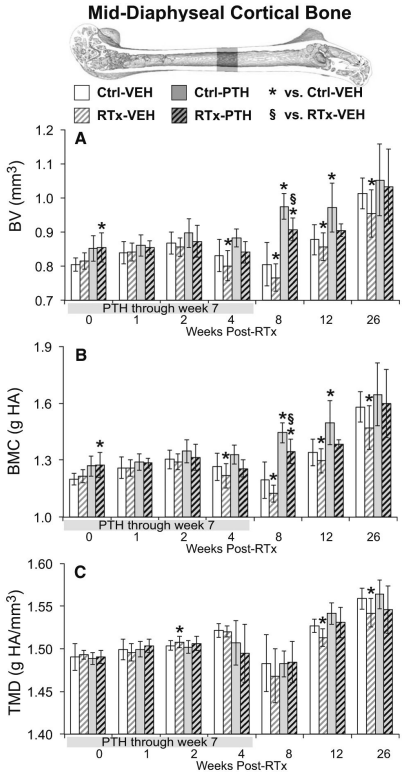

Fig. 2.

Micro-CT analysis of a 1-mm-thick section of mid-diaphyseal femoral cortical bone. **a** The decrease in bone volume (BV) at 4–26 weeks in the RTx-VEH group was prevented by PTH supplementation. **b** Cortical bone mineral content (BMC) responded similarly to bone volume. **c** The decrease in cortical bone tissue mineral density (TMD) in the RTx-VEH group at 12–26 weeks was attenuated in the RTx-PTH group. Data are graphed as average ± standard deviation, with statistical significance indicated at $t < 0.05$ for RTx-VEH vs. Ctrl-VEH or $p < 0.05$ for all other comparisons

Author Manuscript Author Manuscript Author Manuscript Author Manuscript

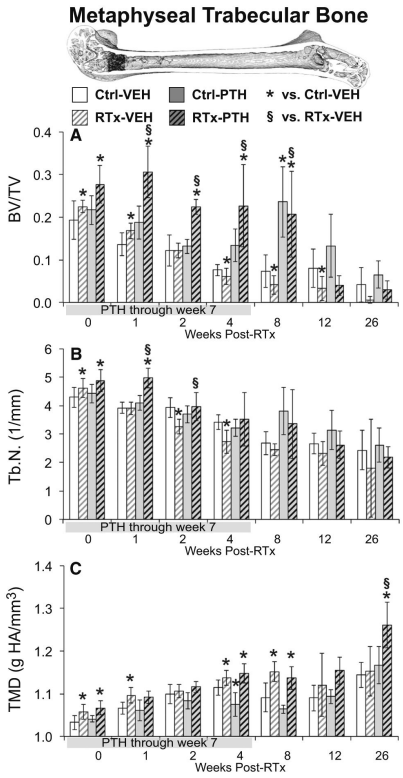

Fig. 3.

Micro-CT analysis of a 0.8-mm-thick volume of metaphyseal trabecular bone located 0.4 mm proximal from the growth plate. **a** Trabecular bone volume fraction (BV/TV) was initially increased in the RTx-VEH group, but decreased from weeks 4–12. Trabecular bone volume was preserved in the RTx-PTH group until cessation of PTH treatment at week seven. **b** Trabecular number (Tb.N) initially increased in response to both RTx and PTH treatment. **c** Trabecular bone tissue mineral density (TMD) increased following RTx, and differed between the RTx-PTH and RTx-VEH groups only at week 26. Data are graphed as average ± standard deviation, with statistical significance indicated at $t < 0.05$ for RTx-VEH vs. Ctrl-VEH or $p < 0.05$ for all other comparisons

Author Manuscript Author Manuscript Author Manuscript Author Manuscript

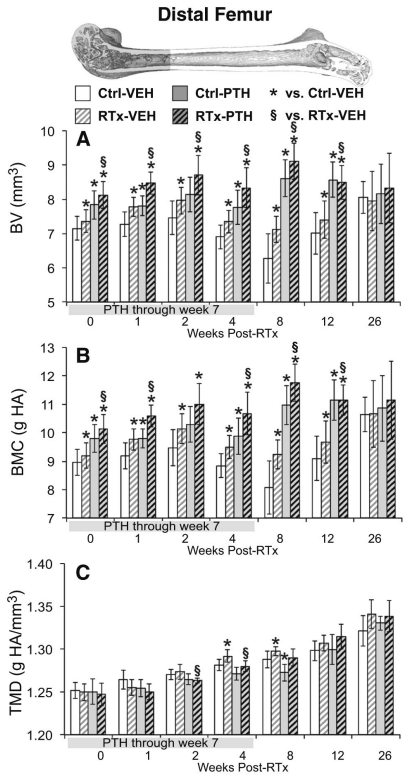

Fig. 4.

Micro-CT analysis of the distal 5-mm femur volume of interest. **a** The distal femur bone volume (BV) was increased in irradiated groups through week 12, though to a greater magnitude in the RTx-PTH group than the VEH-RTx group. **b** Treatment effects on bone mineral content (BMC) paralleled BV responses. **c** Bone tissue mineral density (TMD) was transiently increased in the RTx-VEH group at weeks 4–8. Data are graphed as average ± standard deviation, with statistical significance indicated at $t < 0.05$ for RTx-VEH vs. Ctrl-VEH or $p < 0.05$ for all other comparisons

Author Manuscript Author Manuscript Author Manuscript Author Manuscript

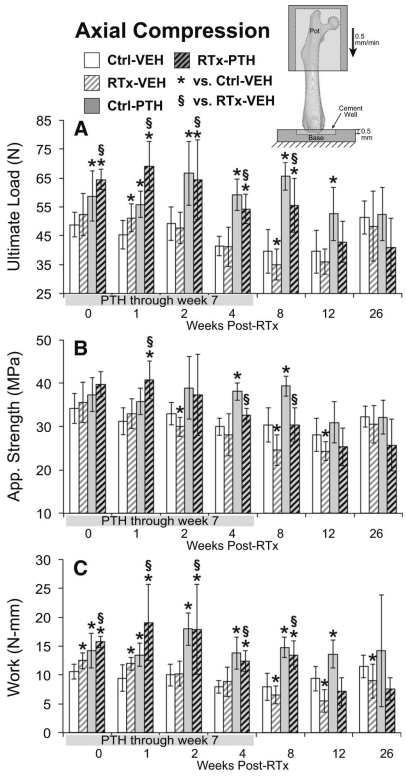

Fig. 5.

Axial compression testing of distal femur. **a** Ultimate load was significantly increased in the PTH-treated groups. **b** Apparent strength was decreased at weeks 2, 8, and 12 in the RTx-VEH group, and PTH treatment attenuated this change. **c** Work to ultimate load initially increased in the RTx-VEH group, then decreased at weeks 8–26. PTH treatment increased work to ultimate load. Data are graphed as average ± standard deviation, with statistical significance indicated at $t < 0.05$ for RTx-VEH vs. Ctrl-VEH or $p < 0.05$ for all other comparisons

Author Manuscript Author Manuscript Author Manuscript Author Manuscript

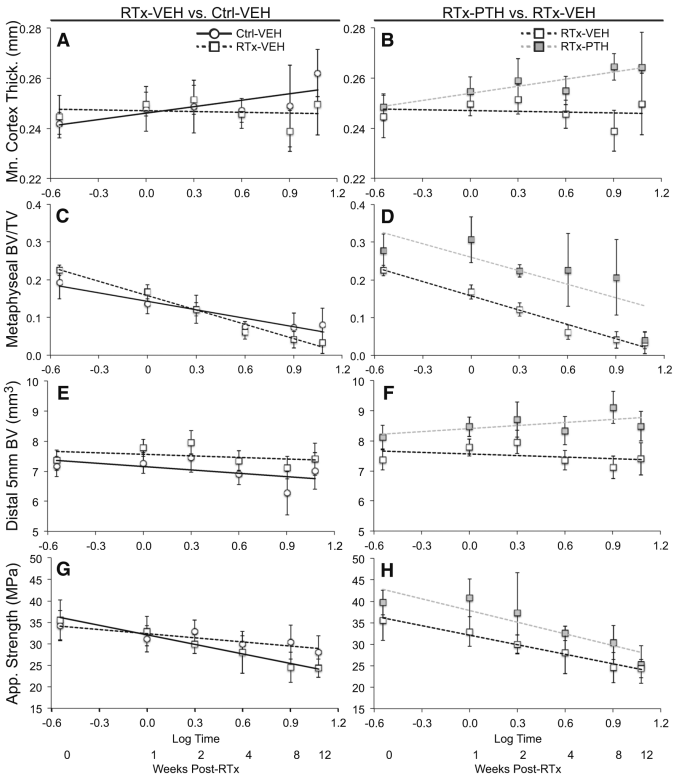

Fig. 6.

Two comparisons were made using ANCOVA analyses with log time as a covariate, excluding the 26-week time point. The effects of radiation on bone (RTx-VEH vs. Ctrl-VEH) are described in the left column for **a** mean cortical thickness, **c** metaphyseal trabecular BV/TV, **e** distal femur bone volume, and **g** apparent strength. The effects of PTH delivery on irradiated limbs (RTx-PTH vs. RTx-VEH) are described in the right column for **b** mean cortical thickness, **d** metaphyseal trabecular BV/TV, **f** distal femur bone volume, and **h** apparent strength. Data are presented as average ± standard deviation vs. Log time

Author Manuscript Author Manuscript Author Manuscript Author Manuscript

Table 1

Results of ANCOVA analyses, calculated using log time and data from the 0–12 week time points only. Radiation damage to bone was verified by making comparisons between the vehicle groups (Ctrl-VEH vs. RTx-VEH). PTH attenuation of radiation damage was assessed by making comparisons between irradiated groups (RTx-PTH vs. RTx-VEH). Data are reported as p values, with arrows indicating the effect of the independent variables on each outcome measure (↑ indicates an increase, ↑ denotes a decrease)

ANCOVAs		**RTx-VEH versus Ctrl-VEH**			**RTx-PTH versus RTx-Ctrl**		
		Log time	**RTx**	**Log time × RTx**	**Log time**	**PTH**	**Log time × PTH**
Diaphyseal Cortex	BV	0.6384	0.1453	0.1484	0.1622	<0.0001↑	0.0136↑
	TMD	0.1059	0.3550	0.2223	0.1892	0.7162	0.3522
	BMC	0.4036	0.1216	0.1091	0.0915	<0.0001↑	0.0112↑
	Mean thickness	0.0606	0.1788	0.0085↓	0.0207↑	<0.0001↑	0.0017↑
	CSA	0.0975	0.2902	0.1539	0.0102↑	<0.0001↑	0.0202↑
Metaphyseal Trabecular	BV/TV	<0.0001↓	0.4958	<0.0001↓	<0.0001	<0.0001↑	0.6251
	Tb.N	<0.0001↓	0.0007↓	0.0033↓	<0.0001	<0.0001↑	0.7415
	Tb.Th	<0.0001↓	<0.0001↑	0.0829	0.6932	<0.0001↑	0.1926
	Tb.Sp	<0.0001↑	0.0002↑	0.0015↑	<0.0001	0.0002↓	0.2183
	TMD	<0.0001↑	0.0001↑	0.3727	<0.0001↑	0.2719	0.6556
	Conn.D	<0.0001↓	0.3731	<0.0001↓	<0.0001↓	<0.0001↑	0.2876
	SMI	<0.0001↑	<0.0001↑	<0.0001↑	<0.0001↑	<0.0001↓	0.0337↓
	DA	0.1023	<0.0001↓	0.0006↓	0.0090↓	0.0132↑	0.3944
Distal 5 mm	BV	0.0030↓	<0.0001↑	0.3640	0.5934	<0.0001↑	0.0065↑
	TMD	<0.0001↑	0.0716	0.0032↑	<0.0001↑	0.0279↓	0.4786
	BMC	0.2376	<0.0001↑	0.2179	0.0021↑	<0.0001↑	0.0025↑
Axial Compression	Ultimate load	<0.0001↓	0.9637	0.0123↓	<0.0001↑	<0.0001↑	0.6334
	Work	<0.0001↓	0.8309	<0.0001↓	<0.0001↓	<0.0001↑	0.5203
	Stiffness	0.0024↑	0.1006	0.0004↑	<0.0001↑	0.8066	0.7059
	Apparent strength	<0.0001↓	0.0135↑	0.0021↑	<0.0001↓	<0.0001↑	0.2456